Title

Rapid degeneration of rod photoreceptors expressing self-association-deficient arrestin-1 mutant

Journal

Cellular Signalling, 25(12)

ISSN

0898-6568

Authors

Song, Xiufeng
Seo, Jungwon
Baameur, Faiza
et al.

Publication Date

2013-12-01

DOI

10.1016/j.cellsig.2013.08.022

Peer reviewed

Published in final edited form as:
Cell Signal. 2013 December ; 25(12): . doi:10.1016/j.cellsig.2013.08.022.

Rapid degeneration of rod photoreceptors expressing self-association-deficient arrestin-1 mutant

Xiufeng Song[1,3], **Jungwon Seo**[1,6,*], **Faiza Baameur**[1,*], **Sergey A. Vishnivetskiy**[1], **Qiuyan Chen**[1], **Seunghyi Kook**[1], **Miyeon Kim**[2,7], **Evan K. Brooks**[2], **Christian Altenbach**[2], **Yuan Hong**[1,8], **Susan M. Hanson**[1,4], **Maria C. Palazzo**[1], **Jeannie Chen**[5], **Wayne L. Hubbell**[2], **Eugenia V. Gurevich**[1], and **Vsevolod V. Gurevich**[1,**]

[1]Vanderbilt University, Nashville, TN 37232

[2]University of California Los Angeles, Los Angeles, CA 90095

[5]University of Southern California, Los Angeles, California 90033

Abstract

Arrestin-1 binds light-activated phosphorhodopsin and ensures timely signal shutoff. We show that high transgenic expression of an arrestin-1 mutant with enhanced rhodopsin binding and impaired oligomerization causes apoptotic rod death in mice. Dark rearing does not prevent mutant-induced cell death, ruling out the role of arrestin complexes with light-activated rhodopsin. Similar expression of WT arrestin-1 that robustly oligomerizes, which leads to only modest increase in the monomer concentration, does not affect rod survival. Moreover, WT arrestin-1 co-expressed with the mutant delays retinal degeneration. Thus, arrestin-1 mutant directly affects cell survival via binding partner(s) other than light-activated rhodopsin. Due to impaired self-association of the mutant its high expression dramatically increases the concentration of the monomer. The data suggest that monomeric arrestin-1 is cytotoxic and WT arrestin-1 protects rods by forming mixed oligomers with the mutant and/or competing with it for the binding to non-receptor partners. Thus, arrestin-1 self-association likely serves to keep low concentration of the toxic monomer. The reduction of the concentration of harmful monomer is an earlier unappreciated biological function of protein oligomerization.

[**]Address correspondence to: Vsevolod V. Gurevich, Department of Pharmacology, Vanderbilt University, Nashville, TN 37232; vsevolod.gurevich@vanderbilt.edu.
[3]Present address: Massachusetts General Hospital Cancer Center, GRJ-904, Boston, MA 02114
[4]Present address: Carroll University, Waukesha, WI 53186
[6]Present address: Wonkwang University, Iksan, Jeollabuk-do, 570-749, South Korea
[7]Present address: Michigan State University, East Lansing, MI 48824
[8]Present address: Drexel University, Philadelphia, PA 19104
[*]These authors equally contributed to this work

Contributors

XS, JS, FB, SAV, QC, SK, MK, EKB, CA, YH, SMH, and MCP performed experiments and contributed to manuscript writing; JC, WLH, EVG, and VVG designed the study, coordinated experiments, and wrote the manuscript. All authors have approved the final article.

Conflict of interest

The authors declare no conflict of interest.

Keywords

Arrestin; self-association; monomer; rhodopsin; cell death; retina; photoreceptors

Introduction

Rod photoreceptors are highly specialized neurons, where light sensitivity is pushed to the physical limit of single photons [1] at the price of expressing very high concentrations of signaling proteins [2] and consuming enormous amounts of energy [3]. This makes rods very sensitive to a variety of genetic and environmental insults, many of which result in retinal degeneration. Defects in important phototransduction, retinoid cycle, metabolic, or structural proteins cause photoreceptor death [4, 5].

Arrestin-1[1] is essential for rapid termination of rhodopsin signaling [6]. Its binding to phosphorylated light-activated rhodopsin (P-Rh*) precludes further transducin activation [7]. Arrestin- 1 is expressed in rods [8–11] and cones [12] at a very high level, sufficient to inactivate virtually all photopigment. Arrestin-1 demonstrates exquisite selectivity to phosphorylated light-activated rhodopsin [13, 14]. Lack of rhodopsin phosphorylation due to the absence of rhodopsin kinase [15] or mutations eliminating rhodopsin phosphorylation sites [16, 17] results in excessive signaling that leads to loss of rod outer segments and rod death. To compensate for phosphorylation defect, we have created transgenic lines expressing arrestin-1-3A (L374A, V375A, F376A) mutant with increased affinity for unphosphorylated light-activated rhodopsin (Rh*) at 50% and 240% of WT level on arrestin-1 knockout (Arr1−/−) background (3A-50$^{arr1-/-}$ and 3A-240$^{arr1-/-}$, respectively). We demonstrated normal light sensitivity and recovery kinetics in single cell recordings and electroretinography (ERG) [18], indicating that arrestin-1-3A successfully replaced missing WT arrestin-1. As expected, in the absence of rhodopsin kinase, both 3A-240$^{arr1-/-}$ and 3A-50$^{arr1-/-}$ lines showed improved rod outer segment morphology and functional performance [18]. However, the amplitudes of ERG a- and bwaves were 30–40% lower in 3A-240$^{arr1-/-}$ animals than in WT and 3A-50$^{arr1-/-}$ line, which parallels the loss of rod photoreceptors seen in 3A-240$^{arr1-/-}$ mice [18].

Here we set out to examine the mechanisms of rod degeneration in 3A-240$^{arr1-/-}$ mice. We found that rod death induced by high levels of arrestin-1-3A mutant, but not wild type (WT) arrestin-1, was age-dependent but light-independent, ruling out the role of arrestin interactions with light-activated rhodopsin. Historically, arrestin-1 studies focused on its interactions with rhodopsin [19]. However, significant amounts of arrestin-1 are invariably detected in rod synaptic terminals [20–22]. Evidence of rhodopsin-independent arrestin-1 functions are only beginning to emerge [22, 23]. In 3A-240$^{arr1-/-}$ mice, rod terminals appear to be affected before massive loss of rods, suggesting a role for arrestin-1- 3A interaction with non-receptor partner(s) in rod death. Importantly, high expression of WT arrestin-1 is not harmful to rods, and co-expression of WT arrestin-1 partially protects against deleterious effects of the mutant.

Materials and methods

Materials

All restriction and DNA modifying enzymes were from New England Biolabs (Ipswich, MA). All other reagents were from Sigma-Aldrich (St. Louis, MO).

[1]We use systematic names of arrestin proteins: arrestin-1 (a.k.a. visual or rod arrestin, 48 kDa protein, or S-antigen), arrestin-2 (β-arrestin or β-arrestin1), arrestin-3 (β-arrestin2 or hTHY-ARRX), and arrestin-4 (cone or X-arrestin).

Transgenic mice expressing WT arrestin-1 and 3A mutant

Animal research was conducted in compliance with the NIH Guide for the Care and Use of Laboratory Animals and approved by the Vanderbilt Institutional Animal Care and Use Committee. WT mouse arrestin-1 and arrestin-1-3A mutant with triple alanine substitution in the C-tail (L374A, V375A, F376A) (that binds Rh* ~10-times better than WT [24]) were transgenically expressed. To this end, the coding sequence with extended 5'- and 3'-UTRs followed by mp1 polyadenylation signal was placed under the control of the pRho4-1 rhodopsin promoter [25] and used to create transgenic mice, as described [9, 10, 18, 19, 26, 27]. All transgenic lines were bred into Arr1−/− background [6] to obtain mice where the mutant is the only arrestin present in photoreceptors. The transgene was maintained in hemizygous state by breeding transgenic lines on Arr1−/− background with transgene-negative Arr1+/+, Arr1+/−, and Arr1−/− mice to obtain necessary control littermates. The expression of transgenic arrestin and rhodopsin was quantified by Western blot in the homogenates of whole eyecups, using the corresponding purified proteins to construct calibration curves [18, 26]. Three transgenic lines WT-120, 3A-50, and 3A-240 expressing WT or 3A arrestin-1 at 120%, 50%, and 240% of WT levels, respectively, on Arr1−/−, Arr1+/−, and Arr1+/+ backgrounds were used in this study.

The analysis of the ONL histology

Mice of either sex were maintained under controlled ambient illumination on a 12 h light/dark cycle. The cages of dark-reared mice were kept in light-proof ventilated boxes from birth, and the husbandry was performed under IR illumination. At indicated ages mice were sacrificed by overdose of isoflurane, the eyes were enucleated and fixed in 4% paraformaldehyde at 4°C overnight, cryoprotected with 30% sucrose in phosphate-buffered saline, pH 7.2 (PBS) for 6 h, and frozen at −80°C. Sections (30 μm) were cut on a cryostat and mounted on polylysine (0.1μg/ml) coated slides. The sections were rehydrated for >40 min in PBS, permeabilized for 10 min in PBS with 0.1% Triton X-100, washed twice for 5 min in PBS, and stained with NeuroTrace 500/525 green fluorescent Nissl (Invitrogen) in PBS (dilution 1:100) for 20 min. The sections were then washed with PBS with 0.1% Triton X-100 for 10 min, and with PBS (2×5 min). Mounted sections were analyzed by confocal microscopy (40 X oil objective) (LSM510; Zeiss, Oberkochen, Germany). The outer nuclear layer (ONL) was visualized by fluorescence in FITC (green) channel, outer segments (OS) were viewed with DIC (phase contrast). Two-channel images were acquired for quantitative analysis. Nissl stains nucleic acids, providing a convenient method of prominently labeling DNA-rich nuclei, yielding characteristic diffuse staining of RNA-rich IS (Figure 1). It also helps to identify nucleic acids-free OS that are clearly visible in DIC image (Figure 3). The images were collected at the depth where all retinal layers were clearly visualized.

The thickness of ONL was measured on green channel images using IPLab Version 3.9.2 (Scanalytics, Inc.). The retinas of at least three mice (three sections per mouse) for each genotype were used. Each side of the section was divided into three segments according to the distance from optical nerve: central, medium, and peripheral in both inferior and superior hemispheres, so that the whole length of the section was divided into six segments. The measurements were performed at five points spaced at equal distances within each segment using the length measurement tool provided by the software. The images were calibrated using the microscope ruler tool, and all measurements were obtained in μm. Average values of each parameter for individual animals were used to calculate the mean and SD for each genotype.

The analysis of the OPL histology

The OPL was stained with rabbit anti-NSF antibody (H-300, Santa Cruz Biotechnology). The 30 μm cryosections were blocked free-floating in PBS/0.3% Triton X- 100/5% BSA for

1 h at room temperature (RT) and then incubated overnight at 4°C with primary antibody at 1:500 dilution. After washing in PBS, sections were incubated with mouse biotinylated antirabbit antibody (Vector Laboratories, 1:200) for 1 h at RT, washed in PBS, and incubated with streptavidin-Alexa-488 (Invitrogen; 1:200) for 1 h at RT. Some sections were counterstained with fluorescent red Nissl NeuroTrace 530/615 (Invitrogen; dilution 1:200) to label nuclear layers. After extensive washing, sections were mounted on Vectabond-coated slides and cover-slipped with Vectashield (both from Vector Laboratories). Mounted sections were imaged by confocal microscopy (LSM510; Zeiss, Oberkochen, Germany). The green channel images were acquired for quantification; dual channel were used for illustration purposes only.

The thickness of OPL was measured using NIS-Elements-AR software (Nikon). The retinal subdivisions were defined as described above for ONL. The measurements were performed at five points spaced at equal distances within each segment. Average values of each parameter for individual animals were used to calculate the mean and SD for each genotype.

Detection of apoptotic cells with Terminal deoxynucleotidyl Transferase (TdT)-mediated dUTP Nick End Labeling (TUNEL)

In Situ Cell Death Detection kit, Fluorescein (Roche) was used following manufacturer's instructions for the TUNEL staining of 30 μm cryosections. The sections were permeabilized by 0.1% Triton-X100 in 0.1% sodium citrate for 90 min, washed in PBS (5 min + 10 min), mounted on slides, and incubated with TUNEL reaction mixture for 60 min at 37°C in a humidified atmosphere in the dark. The samples were washed three times with PBS, air-dried, and immersed into mounting medium with DAPI (Vector laboratories, Inc, CA). Samples were analyzed by fluorescence microscopy. TUNEL-positive cells were detected in FITC (green) channel. Photoreceptor death rate was estimated as the proportion of TUNEL positive cells in the ONL (the number of TUNEL-positive cells divided by the total number of DAPI-stained nuclei). TUNEL-positive cells were counted on the whole length of each section; four sections were examined for each age and genotype to calculate means and SD.

Western blotting

Frozen whole eyecups were homogenized by sonication (sonic dismembrator Model 500, Fisher Scientific, at 30% max power) in 100 mM Tris-HCl, pH 8.0; 2 mM EDTA; 2 mM benzamidine; 1 mM PMSF (dissolved as 100x stock in DMSO). The homogenates were centrifuged for 1 min at 3400 rpm at 4°C in Eppendorf 5417R centrifuge to pellet cell debris. Supernatant was collected, and protein concentration was measured by Bradford Assay (Bio-Rad Laboratories, Hercules, CA). Protein was precipitated by the addition of 9 volumes of methanol, washed with 90% methanol, and dissolved in SDS sample buffer at 0.3μg/μl. Proteins (3 μg/lane) were resolved by 10% SDS-PAGE and transferred to PVDF membrane (Millipore, Bedford, MA). Bands were visualized by appropriate primary antibodies (rabbit polyclonal anti-arrestin antibodies [28]; mouse monoclonal antibodies against Caspases-3, -9, total JNK, phospho-JNK (Cell Signaling Technology) and GAPDH (Ambion)), followed by HRP-conjugated anti-rabbit or anti-mouse secondary antibodies (Jackson Immuno). Protein bands were detected by enhanced chemiluminescence (ECL, Pierce Inc.) followed by exposure to X-ray film. Immunoblots were quantified using QuantityOne software (Bio-Rad Laboratories, Hercules, CA). In case of arrestin-1 and rhodopsin, calibration curves were constructed using known amounts of purified proteins for each blot, as described [18, 26].

Arrestin-1 purification and analysis of its self-association

WT and mutant mouse arrestin-1 were expressed in *E. coli* and purified, as described [29]. All light scattering measurements were made with a DAWN EOS detector coupled to an Optilab T-rEX refractometer (Wyatt Technologies) following gel filtration on a QC-PAK GFC 300 column (7.8mm ID × 15cm) (Tosoh Bioscience). The arrestin samples (100 μl) at different concentrations were incubated in fresh 5 mM DTT for 30 min at room temperature to disrupt covalent inter-arrestin disulfide bonds and injected onto the column at 25°C, at a flow rate of 0.6 ml/min in 50 mM MOPS, pH 7.2, 100 mM NaCl. The column did not resolve oligomeric species, but simply acted as a filter to remove highly scattering particulates. Light scattering at 7 angles (72°–126°), absorbance at 280 nm, and refractive index (at 658 nm) for each sample were taken for a narrow slice centered at the peak of the elution profile [21, 30–32]. The experimental weight-averaged molecular weight values were obtained from the protein concentration and light scattering data using ASTRA 5.3.4.20 software (Wyatt Technologies). The weight-averaged molecular weight data were analyzed using the two-step monomer-dimer-tetramer (MDT) model, as described [21, 30, 31]. The calculations of total arrestin concentration in the OS and IS were performed, as described [26], taking into account that the OS contains about half of the total rod cytoplasm volume [33]. The concentration of the monomer was calculated using total arrestin-1 concentration and measured self-association constants reported in the legend to Fig. 5.

Statistical analysis

StatView software was used for statistical analysis. Most datasets were analyzed by ANOVA with Genotype as main factor separately in central, middle, and peripheral retina. Age effect was analyzed by two-way ANOVA with Genotype and Age as main factors. Post hoc comparisons were made with Bonferroni-Dunn test with correction for multiple comparisons. Unpaired Student's t-test was used for individual comparisons, where appropriate. In all cases, $p<0.05$ was considered significant.

Results

High expression of arrestin-1 mutant induces progressive loss of photoreceptors

The mature retina consists of three nuclear layers and seven major cell types. Cell bodies of rod and cone photoreceptors reside in the outer nuclear layer (ONL), the thickness of which reflects the number of photoreceptor cells. Healthy ONL in WT mice has 9–10 rows of nuclei, with the thickness of >40 μm in the central and middle retina (Fig. 1A,B). The ONL of Arr1−/− mice becomes thinner due to loss of rods, with relatively slow age progression (Fig. 1B). In sharp contrast, the ONL of 3A- $240^{arr1-/-}$ mice expressing high levels of the arrestin-1-3A mutant is significantly thinner than WT as early as 4.5 weeks (in the middle retina), and thinner than that of Arr1−/− at all later ages (Fig. 1B). Progressive ONL thinning in this line reflects rapid photoreceptor death that leaves only one row of nuclei by 32 weeks (Fig. 1A). Interestingly, the layer containing photoreceptor terminals (OPL) also appears much thinner in mice expressing high levels of arrestin-1-3A (Fig. 1A). Importantly, the expression of the same mutant at much lower levels in 3A-$50^{arr1-/-}$ mice does not produce this deleterious effect in younger mice (up to 16 weeks [18]). However, transgene expressed at lower level in 3A-$50^{arr1-/-}$ mice becomes deleterious with age: in mutant mice aged 32 weeks ONL is significantly thinner than in Arr1+/− mice that have comparable level of total arrestin-1 (Fig. 1C,D). The transgene-induced degeneration in older 3A-$50^{arr1-/-}$ mice is significant but still much less evident than in 3A- $240^{arr1-/-}$ of the same age (Fig. 1B,D). Thus, the expression of arrestin-1-3A leads to the progressive loss of photoreceptor cells in a dose- and age-dependent fashion.

Rod death induced by arrestin-1-3A mutant is rhodopsin-independent

Photoreceptor death in mammals can be triggered by light-induced rhodopsin signaling [34] or the formation of tight arrestin-rhodopsin complexes [35, 36]. To test whether light-dependent mechanisms are involved, we reared 3A-240$^{arr1-/-}$ mice in the dark and found the same rate of photoreceptor loss (Fig. 2A,B) and the same proportion of TUNEL-positive apoptotic cells in the ONL (Fig. 2C). Using transgene-negative Arr1−/− littermates as a control, we ascertained that dark rearing protected photoreceptors in these mice, increasing ONL thickness and the length of the outer segments, and reducing the fraction of TUNEL-positive nuclei (Fig. 2), as expected [6, 15]. Thus, in contrast to Arr1- /- animals, photoreceptor death in 3A-240$^{arr1-/-}$ mice is light-independent. WT arrestin-1 demonstrates very low virtually undetectable binding to dark unphosphorylated rhodopsin (Rh) [13, 37], which does not appear to be significantly increased in 3A mutant [18, 24, 32, 38]. Thus, the data suggest that free, rather than rhodopsin-bound arrestin-1-3A induces apoptosis via an earlier unappreciated mechanism.

Apoptotic JNK-independent death mediates the loss of photoreceptors induced by arrestin-1-3A mutant

Two mechanistically distinct modes of cell death, apoptosis and necrosis, have been described. Using terminal deoxynucleotidyl transferase dUTP nick end labeling (TUNEL) we found that photoreceptors in 3A-240$^{arr1-/-}$ mice undergo apoptosis. TUNEL-positive cells show a distinctive ring in the perinuclear area, indicating the labeling of DNA strand breaks (Fig. 3A). We observed virtually no apoptotic cells in WT ONL, and relatively few in Arr1−/− and 3A-50$^{arr1-/-}$ animals (Fig. 3A,B). In contrast, the fraction of TUNEL-positive nuclei in the ONL of 3A-240$^{arr1-/-}$ mice was high at 4 and even higher at 7 weeks, indicative of progressive photoreceptor degeneration (Fig. 3B). Detected rate of apoptosis in this line (Fig. 3B) correlates very well with the thinning of ONL (Fig. 1).

Classical apoptotic pathways involve the activation of caspases, specialized cysteine proteases that cleave at aspartate residues [39]. Caspases fall into two categories: initiator (caspases-2, -8, -9, and – 10) and effector (caspases-3, -6, and –7). Initiator caspases act by cleaving inactive effector procaspases, so that caspase activation manifests itself in the disappearance of the procaspase and the generation of an active caspase of much smaller size [40]. Effector caspases cleave multiple proteins, contributing to the stereotypic morphological and biochemical changes in apoptotic cells [41]. The most common effector enzyme caspase-3 is often activated by caspase-9 in response to cytochrome C release from mitochondria and formation of the apoptosome [42]. The amount of inactive procaspase-9 and procaspase-3 was reduced in eyecup homogenates of 3A-240$^{arr1-/-}$ mice, as compared to WT (Fig. 3C,D,E). The involvement of both caspase-9 and -3 suggests that arrestin-1-3A initiates mitochondria-mediated apoptotic pathway in mouse photoreceptors. Several apoptotic pathways in neurons involve the activation of c-Jun N-terminal kinases (JNKs) [43]. We previously found that arrestin-1 interacts with neuron-specific JNK3 isoform [44] and its upstream kinases [45]. Therefore, we tested the activation (phosphorylation) of JNK3 in retina homogenates and found similar phospho-JNK levels and no measurable JNK3 activation in 3A-240$^{arr1-/-}$ or WT mice (Fig. 3C). Thus, apoptosis induced by arrestin-1-3A does not involve JNK3 activation.

High expression of wild type arrestin-1 does not induce photoreceptor death

The arrestin-1-3A mutant inducing severe photoreceptor loss in the 3A-240$^{arr1-/-}$ line is not deleterious at moderate levels in younger 3A-50$^{arr1-/-}$ animals [18], so that detectable thinning of the ONL appears in animals older than 16 weeks (Fig. 1C,D). Therefore, we tested whether high arrestin-1 expression *per se* is harmful. To this end, we bred a WT arrestin transgene that yields ~120% of WT expression level (WT-120) [11, 27] on arrestin

knockout (WT-120$^{arr1-/-}$), hemizygous (WT-120$^{arr1+/-}$), and WT (WT-120$^{arr1+/+}$) background. The highest expressing line WT-120$^{arr1+/+}$ had virtually the same arrestin-1 level as 3A-240$^{arr1-/-}$ mice (Fig. 4A). All three lines expressing WT arrestin-1 at supra-physiological levels showed very low fraction of TUNEL-positive nuclei in ONL, similar to WT mice (Fig. 4B). In agreement with this finding, mice with elevated WT arrestin-1 levels demonstrate healthy ONL, with the thickness at least equal to that in WT (Fig. 4C). Thus, high level of WT arrestin-1 does not damage photoreceptor cells, suggesting that specific characteristics of arrestin-1-3A mutant are responsible for rod death in 3A-240$^{arr1-/-}$ mice.

Impaired self-association of arrestin-1-3A mutant

Bovine arrestin-1 cooperatively forms dimers and tetramers [21, 46–48], so that at physiological concentrations only a very small fraction exists as a monomer, which is the only active rhodopsin-binding form [21, 30]. We have recently established that mouse and human arrestin-1 also self-associate, attesting to the biological importance of this phenomenon [31]. Therefore, we next examined whether mouse arrestin-1-3A expressed in 3A-240$^{arr1-/-}$ mice is able to oligomerize and found that its self-association is compromised: its dimerization is reduced ($K^{D,dim}$=135+2 μM, as compared to 57.5+0.6 μM for WT) and tetramerization is severely affected ($K^{D,tet}$=380+79 μM, as compared to 63.1+2.6 μM for WT) (Fig. 5). Calculations based on measured dimerization and tetramerization constants of WT mouse arrestin-1 [48], measurements of the relative volumes of rod compartments indicating that the volume of the OS cytoplasm equals that of the rest of the rod [33], and arrestin-1 distribution in rods [8, 11, 20] show that in WT mice in the dark total arrestin-1 concentration in the cell body is ~ 2,000 μM, which translates into ~95 μM monomer. Due to robust self-association, a 2.2-fold increase of total WT arrestin-1 in WT-120$^{arr1+/+}$ mice (to ~ 4,400 μM) results in only a modest increase in free monomer to ~104 μM. Decreased self-association in case of 3A mutant at ~50% of normal expression in 3A-50$^{arr1-/-}$ line yields ~115 μM monomer (based on constants measured in the experiments shown in Fig. 5), which rods apparently tolerate fairly well (Fig. 1C,D; see also [18]). In 3A-240$^{arr1-/-}$ mice expressing 3A mutant Arr1 at a total level of ~4,800 μM, the concentration of the monomer in the cell body reaches ~270 μM, almost 3-fold higher than in WT-120$^{arr1+/+}$ mice with similar total arrestin expression.

Synaptic terminals of rods expressing arrestin-1-3A show early damage

Arrestin-1 binding to N-ethylmaleimide-sensitive factor (NSF) was recently shown to play an important role in the maintenance of rod synaptic terminals [22]. Apparent age-dependent reduction of the OPL in 3A-240$^{arr1-/-}$ animals is noticeable on Nissl-stained section (Fig. 1A) indicating the possibility that high expression of the mutant affects synaptic terminals. Therefore, we analyzed the thickness of the OPL (visualized with anti-NSF antibody) in WT, Arr1−/−, and 3A-240$^{arr1-/-}$ mice as a function of age up to 32 weeks (Fig. 6). In agreement with the report that the absence of arrestin-1 damages rod synapses [22], we found that the OPL in Arr1−/− mice is much thinner than in WT animals, and is progressively reduced with age. The OPL in 3A-240$^{arr1-/-}$ mice is even thinner than in Arr1−/− animals in the middle and peripheral retina (Fig. 6A,B). In fact, the OPL appears to deteriorate at least as fast as the ONL (significant damage detected in all retinal subdivisions at 4 weeks; Figs. 1 and 6), suggesting that the damage to synaptic terminals might trigger photoreceptor demise.

Co-expression of wild type arrestin-1 protects against 3A mutant

In 3A-240$^{arr1-/-}$ animals, 3A mutant is the only form of arrestin-1 present in rods. The solution tetramer of arrestin-1 has the shape of a “closed” diamond, where each protomer interacts with two “sister” subunits via two distinct interfaces [30]. This model predicts that any form of arrestin-1 where only one of these interfaces is damaged by mutagenesis can

interact with another arrestin-1 molecule via the second interface. Indeed, we previously found that WT arrestin-1 can recruit oligomerization-deficient mutants into mixed oligomers [21, 30], which would reduce the concentration of free mutant monomer. Therefore, we tested whether co-expression of "harmless" WT arrestin-1 can affect the action of the mutant. To this end, we generated lines expressing 3A transgene on Arr1+/+ background, where WT and mutant arrestin-1 were both present in rods. We found that WT arrestin-1 co-expressed with the mutant increases the number of surviving rods, as revealed by thicker ONL both at 4 and 7 weeks (Fig. 7A,B), even though the total level of arrestin-1 in 3A-240$^{arr1+/+}$ mice is even greater than in 3A-240$^{arr1-/-}$ animals. This protective effect gradually wears off: the difference with 3A-240$^{arr1-/-}$ mice is significant at 4 weeks (at this age, 3A-240$^{arr1+/+}$ mice are not different from WT), smaller at 7 weeks (Fig. 7B), and disappears thereafter. Thus, co-expression of WT arrestin-1, even though it further increases total arrestin-1 concentration, protects photoreceptors against 3A-induced damage, prolonging their survival. These data suggest that the two forms of arrestin-1 do not act independently of each other, but functionally interact in mouse photoreceptors and/or compete for non-rhodopsin binding partner(s).

Co-expression of WT arrestin-1 with the 3A mutant prolonged rod survival (Fig. 7). Therefore, we tested whether it protects rod synapses as well, again comparing 3A-240$^{arr1-/-}$ and 3A-240$^{arr1+/+}$ animals, and found that WT arrestin-1 dramatically reduces the thinning of the OPL (Fig. 8A,B). Protective effect of WT arrestin-1 is evident at both 4 and 7 weeks, although it is more pronounced at an earlier age. In contrast to 3A-240$^{arr1-/-}$ animals, OPL thickness in the retina of 3A-240$^{arr1+/+}$ mice is indistinguishable from WT at 4 weeks, and remains essentially normal even at 7 weeks in the middle and peripheral retina (Fig. 8B).

Discussion

Single photon sensitivity of rods [1] requires concentrations of signaling proteins that are 1,000–10,000 times higher than in other cells. The expression of ~3 mM rhodopsin, >2 mM arrestin-1, ~0.3 mM transducin, and high levels of other signaling proteins [2] makes rods extremely sensitive to genetic and environmental insults. Here we describe a novel light-independent mechanism of photoreceptor death induced by oligomerization-deficient arrestin-1-3A mutant.

Excessive rhodopsin signaling induced by bright light or defects in the shutoff mechanism [6, 15, 16] triggers photoreceptor demise [34]. Stable arrestin-rhodopsin complexes were shown to induce apoptosis in *Drosophila* [49, 50] and mammalian [35, 36] photoreceptors. Biochemical balance in rods is so precarious that even over-expression of normal proteins can be harmful, as an excellent correlation between transgenic expression of WT opsin and the severity of photoreceptor degeneration shows [51]. However, supra-physiological expression of WT arrestin-1 is harmless (Fig. 4; [11]), whereas arrestin-1-3A induces rod death in a concentration-dependent manner (Fig. 1).

Significant functional differences between WT arrestin-1 and arrestin-1-3A can underlie mutant cytotoxicity. The basal arrestin conformation is stabilized by intra-molecular interactions [52–55], which are disrupted by activated phosphoreceptors [56]. Mutations disrupting these interactions "preactivate" arrestin-1 and greatly increase its binding to unphosphorylated Rh* [24, 32, 38, 57], allowing arrestin-1 mutants to quench the signaling of Rh* *in vitro* [58] and *in vivo* [18]. Arrestin-1-3A also binds P-Rh* better than WT [18, 24, 32, 59]. However, in sharp contrast to Arr1−/− mice, dark rearing does not protect rods in 3A-240$^{arr1-/-}$ animals (Fig. 2). Taken together with the evidence that 3A mutation does not noticeably increase arrestin-1 binding to dark Rh [18, 24, 32, 38], the only rhodopsin

form present in dark-reared animals, this finding suggests that arrestin-1-3A does not act via rhodopsin binding.

Three lines of evidence argue against the possibility that transgene in 3A-240$^{arr1-/-}$ line simply disrupted a gene necessary for rod survival. First, an independent 3A-50$^{arr1-/-}$ transgenic line expressing the same mutant at a lower level shows slow loss of rods (Fig. 1), indicating that arrestin-1-3A per se is the culprit. Second, transgenic mice used here were hemizygous, carrying perfectly normal second allele, so the disruption of any gene would yield observed dramatic phenotype only in case of severe haplo-insufficiency. Third, co-expression of WT arrestin-1 protects rods (Figs. 7,8), which would be virtually impossible if the transgene disrupted an unrelated gene.

The dose-dependence of the 3A arrestin-1 effect on arrestin-1 null background suggests gain-of-function. Conceivably, arrestin-1 binding to a non-rhodopsin partner is necessary for rod health, whereas 3A mutant could form structurally or functionally different complexes with it that are cytotoxic. These interactions might occur in synaptic terminals resulting in their special vulnerability, which is consistent with our data (Figs. 6,8). So far, NSF was the only arrestin-1-interacting protein reported to be involved in rod maintenance [22], and it is localized to synaptic terminals, being involved in exocytosis of the neurotransmitters. This interaction appears beneficial for the rod [22], but it is possible that excessive binding is harmful. Abnormal interaction of arrestin-1-3A with nonrhodopsin partners would also explain protection by WT arrestin-1: it can out-compete the mutant, reducing the number of harmful complexes. The recruitment of clathrin adaptor AP2 via the C-tail of WT arrestin-1, which is released upon rhodopsin binding [60, 61], was recently shown to cause rod loss [36]. The C-tail of the 3A mutant is constitutively released, suggesting that it can harm rods by depleting AP2.

Microtubule binding may also mediate toxic effect of arrestin-1-3A, since it has higher affinity than WT [20] and might saturate microtubules, hampering their normal function. Upon illumination, arrestin-1 moves to the OS due to rhodopsin binding [20] at 1:1 molar ratio [21, 62–67]. Therefore, light-dependent translocation exacerbates the difference between 3A-240$^{arr1-/-}$ and 3A-50$^{arr1-/-}$ mice. In the dark, arrestin-1-3A in both lines predominantly localizes to the IS, like WT [20, 21]. The excess of rhodopsin over arrestin-1 in WT and 3A-50$^{arr1-/-}$ mice enables virtually complete translocation [20], reducing arrestin-1 levels in cell body in the light. The situation in 3A-240$^{arr1-/-}$ mice is dramatically different: due to large excess over rhodopsin only a fraction of arrestin-1 translocates, so high concentration of arrestin-1-3A persists in cell body even in bright light [21]. However, it appears unlikely that abnormal interaction with microtubules causes rod death. First, similarly high expression of WT arrestin-1 (Fig. 4), which also binds microtubules [20, 68, 69], does not harm photoreceptors (Fig. 4; [26]). Second, the expression of arrestin-1-3A on Arr1+/+ background that increases total arrestin-1, which reduces the proportion of arrestin-1 translocating to the OS [21] and likely further clog microtubules, nevertheless protects photoreceptors (Figs. 7,8). Thus, neither incomplete arrestin-1 translocation *per se* nor excessive microtubule binding harms the rods.

Functional interplay between the two forms of arrestin-1 suggests the involvement of a process where they physically interact. This points to arrestin self-association, observed in bovine [21, 30, 46, 47], mouse [31], and human [31] arrestin-1. It is the only known biochemical mechanism of crosstalk between arrestin-1 molecules. Biological role of arrestin-1 self-association remains unknown. Oligomerization of mouse arrestin-1-3A is compromised (Fig. 5), identifying a likely reason for its cytotoxicity. This model explains protection by WT arrestin-1 (Figs. 7,8), which recruits oligomerization-deficient mutants into tetramers [21, 30]. Due to robust self-association of WT arrestin-1, ~2.2-fold higher

expression in WT-120$^{arr1+/+}$ animals than in WT mice yields a modest ~17% increase in free monomer to ~104 μM. In contrast, in 3A-240$^{arr1-/-}$ mice expected concentration of monomer is ~270 μM, which is almost three times higher than in WT mice (~95 μM). Oligomerization-deficient arrestin-1-3A in 3A-50$^{arr1-/-}$ line yields ~115 μM monomer, which rods tolerate for several months (Fig. 1)[18]. Apparently, co-expressed WT arrestin-1 in 3A-240$^{arr1+/+}$ line does not reduce the monomer concentration to a safe level, as the protection is transient, decreasing with age (Figs. 7,8). The cytotoxicity of monomeric arrestin provides the most parsimonious interpretation of our data. It explains why high expression of oligomerization-deficient arrestin-1-3A causes rod loss (Figs. 1–4, 6–8), while mild toxicity of low level of the same protein is only detectable at older ages (Fig. 1)[18], whereas high expression of WT arrestin-1 is harmless (Fig. 4)[26]. Arrestin- 1-3A mutant demonstrates gain of function, e.g., it does something that WT arrestin-1 does not do. Thus, regardless of the mechanism whereby it harms rods, which might involve the interactions with AP2, NFS, microtubules, or some other partner, only a process that takes it out of action can suppress its effects. Therefore, reduction of monomer levels via recruitment of self-association-deficient mutants by WT arrestin-1 into mixed oligomers [21] is the most logical explanation of observed protection (Figs. 7,8).

Monomer toxicity, along with the fact that rods need enough arrestin-1 to quench all rhodopsin to ensure survival in bright light during the day [45, 70], provides the first satisfactory explanation for arrestin-1 self-association. The structure of oligomers, where identified receptor-binding surfaces [60, 71–74] are shielded by sister subunits [30], and the disappearance of all inter-subunit distances upon binding to P-Rh* [21], demonstrate that only monomer binds rhodopsin. Thus, unlike other rod proteins, arrestin-1 is stored in the form of inactive oligomer. While mouse, bovine, and human arrestin-1 exist in a monomer-dimer-tetramer equilibrium, their self-association constants are quite different [31]. The fraction of the monomer is inversely proportional to the longevity of the species, being the highest in mice and lowest in humans, suggesting that the longer photoreceptors must live, the lower allowable monomer concentration.

Monomer toxicity also explains the ratio of the two arrestin subtypes in cones. Vertebrates express two visual arrestins, until recently conveniently classified as “rod” (arrestin-1) and “cone” (arrestin-4). Arrestin-4 is perfectly suited for photoreceptors operating at high rate of photopigment bleaching: unlike other subtypes, arrestin-4 forms relatively short-lived complexes with the receptor [54], which allows rapid recycling of cone opsins for immediate reuse. Low expression of arrestin-4 [75] and the finding that arrestin-1 outnumbers arrestin-4 in mouse cones by ~50:1 [12] shattered commonly held ideas regarding arrestin specialization. Vertebrate cones had their own dedicated subtype for hundreds of millions of years [76]. No plausible explanation for arrestin-1 presence in cones has been proposed. Cones, like rods, need enough arrestin to quench virtually all photopigment. If monomer is toxic, cones simply cannot afford to express self-association-deficient arrestin-4 [77] in sufficient quantities. Therefore, cones keep their main stock in the form of arrestin-1. Arrestin-1 might make arrestin-4 safer by forming mixed oligomers, but this remains to be elucidated.

Our unexpected finding also suggests that therapeutically usable enhanced mutants compensating for the defects of rhodopsin phosphorylation [18, 32, 59] should either readily self-associate, or be expressed at safe low levels. Our results suggest that oligomerization of non-visual arrestin-2 [78, 79], expressed in mature neurons at much higher levels than in dividing cells [80, 81], may also serve to prevent monomer toxicity. The reduction of the concentration of harmful monomer is an earlier unappreciated physiological function of protein oligomerization. It is tempting to speculate that our findings apply to other cases where the role self-association of various proteins remains unclear.

The identification of binding partner that mediates cytotoxicity of monomeric arrestin-1 requires further investigation. It is also possible that arrestin-1 binds multiple non-rhodopsin partners, particularly in synaptic terminals, and the excess of one or more of these interactions triggers rod death.

Conclusions

- Oligomerization-deficient arrestin-1-3A mutant causes rod death in a concentration-dependent manner.
- The effects of arrestin-1-3A are light-independent.
- Very high expression of WT arrestin-1 does not harm the rods.
- Co-expression of WT arrestin-1 partially protects rods against deleterious effects of the mutant.
- Monomeric arrestin-1 is toxic, and its robust self-association is a cytoprotective mechanism.

Acknowledgments

Supported by NIH grants EY011500 (VVG), NS045117 (EVG), EY05216 and the Jules Stein Professorship Endowment (WLH), EY012155 (JC), and P30 core grant in vision research EY008126 (to Vanderbilt University). We are grateful to Drs. L. A. Donoso, R. S. Molday, and C.M. Craft for monoclonal anti-arrestin and anti-rhodopsin antibodies, and mouse rod arrestin cDNA, respectively, and to Frances Y. Cheng for technical assistance.

Abbreviations

GPCR	G protein-coupled receptor
GRK	G protein-coupled receptor kinase
WT	wild type
Rh	dark unphosphorylated rhodopsin
Rh*	light-activated unphosphorylated rhodopsin
P-Rh	dark phosphorylated rhodopsin
P-Rh*	light-activated phosphorylated rhodopsin
P-Ops	phospho-opsin.

References

1. Baylor DA, Lamb TD, Yau KW. J Physiol. 1979; 288:613–634. [PubMed: 112243]
2. Pugh, EN., Jr; Lamb, TD. Handbook of Biological Physics. Molecular Mechanisms in Visual Transduction. Stavenga, DG.; DeGrip, WJ.; Pugh, EN., Jr, editors. Amsterdam: Elsevier; 2000. p. 183-255.
3. Linton JD, Holzhausen LC, Babai N, Song H, Miyagishima KJ, Stearns GW, Lindsay K, Wei J, Chertov AO, Peters TA, Caffe R, Pluk H, Seeliger MW, Tanimoto N, Fong K, Bolton L, Kuok DL, Sweet IR, Bartoletti TM, Radu RA, Travis GH, Zagotta WN, Townes-Anderson E, Parker E, Van der Zee CE, Sampath AP, Sokolov M, Thoreson WB, Hurley JB. Proc Natl Acad Sci U S A. 2010; 107:8599–8604. [PubMed: 20445106]
4. Hartong DT, Berson EL, Dryja TP. Lancet. 2006; 368:1795–1809. [PubMed: 17113430]
5. Sancho-Pelluz J, Arango-Gonzalez B, Kustermann S, Romero FJ, van Veen T, Zrenner E, Ekström P, Paquet-Durand F. Mol Neurobiol. 2008; 38:253–269. [PubMed: 18982459]

6. Xu J, Dodd RL, Makino CL, Simon MI, Baylor DA, Chen J. Nature. 1997; 389:505–509. [PubMed: 9333241]
7. Krupnick JG, Gurevich VV, Benovic JL. J Biol Chem. 1997; 272:18125–18131. [PubMed: 9218446]
8. Strissel KJ, Sokolov M, Trieu LH, Arshavsky VY. J Neurosci. 2006; 26:1146–1153. [PubMed: 16436601]
9. Hanson SM, Gurevich EV, Vishnivetskiy SA, Ahmed MR, Song X, Gurevich VV. Proc Nat Acad Sci USA. 2007; 104:3125–3128. [PubMed: 17360618]
10. Nair KS, Hanson SM, Mendez A, Gurevich EV, Kennedy MJ, Shestopalov VI, Vishnivetskiy SA, Chen J, Hurley JB, Gurevich VV, Slepak VZ. Neuron. 2005; 46:555–567. [PubMed: 15944125]
11. Song X, Vishnivetskiy SA, Seo J, Chen J, Gurevich EV, Gurevich VV. Neuroscience. 2011; 174:37–49. [PubMed: 21075174]
12. Nikonov SS, Brown BM, Davis JA, Zuniga FI, Bragin A, Pugh ENJ, Craft CM. Neuron. 2008; 59:462–474. [PubMed: 18701071]
13. Gurevich VV, Benovic JL. J Biol Chem. 1993; 268:11628–11638. [PubMed: 8505295]
14. Gurevich VV, Benovic JL. J. Biol. Chem. 1995; 270:6010–6016. [PubMed: 7890732]
15. Chen CK, Burns ME, Spencer M, Niemi GA, Chen J, Hurley JB, Baylor DA, Simon MI. Proc Nat Acad Sci USA. 1999; 96:3718–3722. [PubMed: 10097103]
16. Chen J, Makino CL, Peachey NS, Baylor DA, Simon MI. Science. 1995; 267:374–377. [PubMed: 7824934]
17. Mendez A, Burns ME, Roca A, Lem J, Wu LW, Simon MI, Baylor DA, Chen J. Neuron. 2000; 28:153–164. [PubMed: 11086991]
18. Song X, Vishnivetskiy SA, Gross OP, Emelianoff K, Mendez A, Chen J, Gurevich EV, Burns ME, Gurevich VV. Curr Biol. 2009; 19:700–705. [PubMed: 19361994]
19. Cleghorn WM, Tsakem EL, Song X, Vishnivetskiy SA, Seo J, Chen J, Gurevich EV, Gurevich VV. PLoS One. 2011; 6:e22797. [PubMed: 21818392]
20. Nair KS, Hanson SM, Mendez A, Gurevich EV, Kennedy MJ, Shestopalov VI, Vishnivetskiy SA, Chen J, Hurley JB, Gurevich VV, Slepak VZ. Neuron. 2005; 46:555–567. [PubMed: 15944125]
21. Hanson SM, Van Eps N, Francis DJ, Altenbach C, Vishnivetskiy SA, Klug CS, Hubbell WL, Gurevich VV. EMBO J. 2007; 26:1726–1736. [PubMed: 17332750]
22. Huang SP, Brown BM, Craft CM. J Neurosci. 2010; 30:9381–9391. [PubMed: 20631167]
23. Smith WC, Bolch SN, Dugger DR, Li J, Esquenazi I, Arendt A, Benzenhafer D, McDowell JH. Invest Ophthalmol Vis Sci. 2011; 52:1832–1840. [PubMed: 21051714]
24. Gurevich VV. J Biol Chem. 1998; 273:15501–15506. [PubMed: 9624137]
25. Lem J, Applebury ML, Falk JD, Flannery JG, Simon MI. Neuron. 1991; 6:201–210. [PubMed: 1825171]
26. Song X, Vishnivetskiy SA, Seo J, Chen J, Gurevich EV, Gurevich VV. Neuroscience. 2011; 174:37–49. [PubMed: 21075174]
27. Burns ME, Mendez A, Chen CK, Almuete A, Quillinan N, Simon MI, Baylor DA, Chen J. J Neurosci. 2006; 26:1036–1044. [PubMed: 16421323]
28. Song X, Gurevich EV, Gurevich VV. J Neurochem. 2007; 103:1053–1062. [PubMed: 17680991]
29. Gurevich VV, Benovic JL. Methods Enzymol. 2000; 315:422–437. [PubMed: 10736718]
30. Hanson SM, Dawson ES, Francis DJ, Van Eps N, Klug CS, Hubbell WL, Meiler J, Gurevich VV. Structure. 2008; 16:924–934. [PubMed: 18547524]
31. Kim M, Hanson SM, Vishnivetskiy SA, Song X, Cleghorn WM, Hubbell WL, Gurevich VV. Biochemistry. 2011; 50:2235–2242. [PubMed: 21288033]
32. Vishnivetskiy SA, Chen Q, Palazzo MC, Brooks EK, Altenbach C, Iverson TM, Hubbell WL, Gurevich VV. J Biol Chem. 2013; 288:3394–3404. [PubMed: 23250748]
33. Peet JA, Bragin A, Calvert PD, Nikonov SS, Mani S, Zhao X, Besharse JC, Pierce EA, Knox BE, Pugh ENJ. J Cell Sci. 2004; 117:3049–3059. [PubMed: 15197244]

34. Hao W, Wenzel A, Obin MS, Chen CK, Brill E, Krasnoperova NV, Eversole-Cire P, Kleyner Y, Taylor A, Simon MI, Grimm C, Remé CE, Lem J. Nat Genet. 2002; 32:254–260. [PubMed: 12219089]
35. Chen J, Shi G, Concepcion FA, Xie G, Oprian D, Chen J. J Neurosci. 2006; 26:11929–11937. [PubMed: 17108167]
36. Moaven H, Koike Y, Jao CC, Gurevich VV, Langen R, Chen J. Proc Natl Acad Sci U S A. 2013; 110:9463–9468. [PubMed: 23690606]
37. Gurevich VV, Benovic JL. J Biol Chem. 1992; 267:21919–21923. [PubMed: 1400502]
38. Vishnivetskiy SA, Schubert C, Climaco GC, Gurevich YV, Velez M-G, Gurevich VV. J Biol Chem. 2000; 275:41049–41057. [PubMed: 11024026]
39. Thornberry NA, Lazebnik Y. Science. 1998; 281:1312–1316. [PubMed: 9721091]
40. Boatright KM, Renatus M, Scott FL, Sperandio S, Shin H, Pedersen IM, Ricci JE, Edris WA, Sutherlin DP, Green DR, Salvesen GS. Mol Cell. 2003; 11:529–541. [PubMed: 12620239]
41. Fischer U, Janicke RU, Schulze-Osthoff K. Cell Death Differ. 2003; 10:76–100. [PubMed: 12655297]
42. Danial NN, Korsmeyer SJ. Cell. 2004; 116:205–219. [PubMed: 14744432]
43. Yuan J, Yankner BA. Nature. 2000; 407:802–809. [PubMed: 11048732]
44. Song X, Raman D, Gurevich EV, Vishnivetskiy SA, Gurevich VV. J Biol Chem. 2006; 281:21491–21499. [PubMed: 16737965]
45. Gurevich VV, Hanson SM, Song X, Vishnivetskiy SA, Gurevich EV. Prog Retin Eye Res. 2011; 30:405–430. [PubMed: 21824527]
46. Schubert C, Hirsch JA, Gurevich VV, Engelman DM, Sigler PB, Fleming KG. J Biol Chem. 1999; 274:21186–21190. [PubMed: 10409673]
47. Imamoto Y, Tamura C, Kamikubo H, Kataoka M. Biophys J. 2003; 85:1186–1195. [PubMed: 12885662]
48. Kim M, Hanson SM, Vishnivetskiy SA, Song X, Cleghorn WM, Hubbell WL, Gurevich VV. Biochemistry. 2011; 50:2235–2242. [PubMed: 21288033]
49. Alloway PG, Howard L, Dolph PJ. Neuron. 2000; 28:129–138. [PubMed: 11086989]
50. Kiselev A, Socolich M, Vinos J, Hardy RW, Zuker CS, Ranganathan R. Neuron. 2000; 28:139–152. [PubMed: 11086990]
51. Tan E, Wang Q, Quiambao AB, Xu X, Qtaishat NM, Peachey NS, Lem J, Fliesler SJ, Pepperberg DR, Naash MI, Al-Ubaidi MR. Invest Ophthalmol Vis Sci. 2001; 42:589–600. [PubMed: 11222515]
52. Hirsch JA, Schubert C, Gurevich VV, Sigler PB. Cell. 1999; 97:257–269. [PubMed: 10219246]
53. Han M, Gurevich VV, Vishnivetskiy SA, Sigler PB, Schubert C. Structure. 2001; 9:869–880. [PubMed: 11566136]
54. Sutton RB, Vishnivetskiy SA, Robert J, Hanson SM, Raman D, Knox BE, Kono M, Navarro J, Gurevich VV. J Mol Biol. 2005; 354:1069–1080. [PubMed: 16289201]
55. Zhan X, Gimenez LE, Gurevich VV, Spiller BW. J Mol Biol. 2011; 406:467–478. [PubMed: 21215759]
56. Gurevich VV, Gurevich EV. Trends Pharmacol Sci. 2004; 25:105–111. [PubMed: 15102497]
57. Vishnivetskiy SA, Paz CL, Schubert C, Hirsch JA, Sigler PB, Gurevich VV. J Biol Chem. 1999; 274:11451–11454. [PubMed: 10206946]
58. Gray-Keller MP, Detwiler PB, Benovic JL, Gurevich VV. Biochemistry. 1997; 36:7058–7063. [PubMed: 9188704]
59. Vishnivetskiy SA, Baameur F, Findley KR, Gurevich VV. J Biol Chem. 2013; 288:11741–11750. [PubMed: 23476014]
60. Hanson SM, Francis DJ, Vishnivetskiy SA, Kolobova EA, Hubbell WL, Klug CS, Gurevich VV. Proc Natl Acad Sci U S A. 2006; 103:4900–4905. [PubMed: 16547131]
61. Vishnivetskiy SA, Francis DJ, Van Eps N, Kim M, Hanson SM, Klug CS, Hubbell WL, Gurevich VV. J. Mol. Biol. 2010; 395:42–54. [PubMed: 19883657]

62. Bayburt TH, Vishnivetskiy SA, McLean M, Morizumi T, Huang CC, Tesmer JJ, Ernst OP, Sligar SG, Gurevich VV. J Biol Chem. 2011; 286:1420–1428. [PubMed: 20966068]
63. Tsukamoto H, Sinha A, Dewitt M, Farrens DL. J Mol Biol. 2010; 399:501–511. [PubMed: 20417217]
64. Kim M, Vishnivetskiy SA, Van Eps N, Alexander NS, Cleghorn WM, Zhan X, Hanson SM, Morizumi T, Ernst OP, Meiler J, Gurevich VV, Hubbell WL. Proc Nat Acad Sci USA. 2012; 109:18407–18412. [PubMed: 23091036]
65. Zhuang T, Chen Q, Cho M-K, Vishnivetskiy SA, Iverson TI, Gurevich VV, Hubbell WL. Proc Nat Acad Sci USA. 2013; 110:942–947. [PubMed: 23277586]
66. Vishnivetskiy SA, Ostermaierm MK, Singhal A, Panneels V, Homan KT, Glukhova A, Sligar SG, Tesmer JJ, Schertler GF, Standfuss J, Gurevich VV. Cell Signal. 2013; 25:2155–2162. [PubMed: 23872075]
67. Singhal A, Ostermaier MK, Vishnivetskiy SA, Panneels V, Homan KT, Tesmer JJ, Veprintsev D, Deupi X, Gurevich VV, Schertler GF, Standfuss J. EMBO Rep. 2013; 14:520–526. [PubMed: 23579341]
68. Nair KS, Hanson SM, Kennedy MJ, Hurley JB, Gurevich VV, Slepak VZ. J Biol Chem. 2004; 279:41240–41248. [PubMed: 15272005]
69. Hanson SM, Francis DJ, Vishnivetskiy SA, Klug CS, Gurevich VV. J Biol Chem. 2006; 281:9765–9772. [PubMed: 16461350]
70. Sommer ME, Hofmann KP, Heck M. Nature communications. 2012; 3:995.
71. Vishnivetskiy SA, Hosey MM, Benovic JL, Gurevich VV. J. Biol. Chem. 2004; 279:1262–1268. [PubMed: 14530255]
72. Hanson SM, Gurevich VV. J Biol Chem. 2006; 281:3458–3462. [PubMed: 16339758]
73. Gimenez LE, Vishnivetskiy SA, Baameur F, Gurevich VV. J Biol Chem. 2012; 287:29495–29505. [PubMed: 22787152]
74. Vishnivetskiy SA, Gimenez LE, Francis DJ, Hanson SM, Hubbell WL, Klug CS, Gurevich VV. J Biol Chem. 2011; 286:24288–24299. [PubMed: 21471193]
75. Chan S, Rubin WW, Mendez A, Liu X, Song X, Hanson SM, Craft CM, Gurevich VV, Burns ME, Chen J. Invest Ophthalmol Vis Sci. 2007; 48:1968–1075. [PubMed: 17460248]
76. Gurevich EV, Gurevich VV. Genome Biol. 2006; 7:236. [PubMed: 17020596]
77. Hanson SM, Vishnivetskiy SA, Hubbell WL, Gurevich VV. Biochemistry. 2008; 47:1070–1075. [PubMed: 18161994]
78. Storez H, Scott MG, Issafras H, Burtey A, Benmerah A, Muntaner O, Piolot T, Tramier M, Coppey-Moisan M, Bouvier M, Labbé-Jullié C, Marullo S. J Biol Chem. 2005; 280:40210–40215. [PubMed: 16199535]
79. Milano SK, Kim YM, Stefano FP, Benovic JL, Brenner C. J Biol Chem. 2006; 281:9812–9823. [PubMed: 16439357]
80. Gurevich EV, Benovic JL, Gurevich VV. J Neurochem. 2004; 91:1404–1416. [PubMed: 15584917]
81. Gurevich EV, Benovic JL, Gurevich VV. Neuroscience. 2002; 109:421–436. [PubMed: 11823056]

Highlights

- Monomeric arrestin-1 is cytotoxictoxic.
- Robust self-association of arestin-1 is a cytoprotective mechanism.
- Cytotoxicity of monomer of naturally oligomerization-deficient cone arrestin-4 might explain why cones express 50-fold more arrestin-1 than arrestin-4.
- Monomer toxicity might be the reason for self-association of non-visual arrestins.

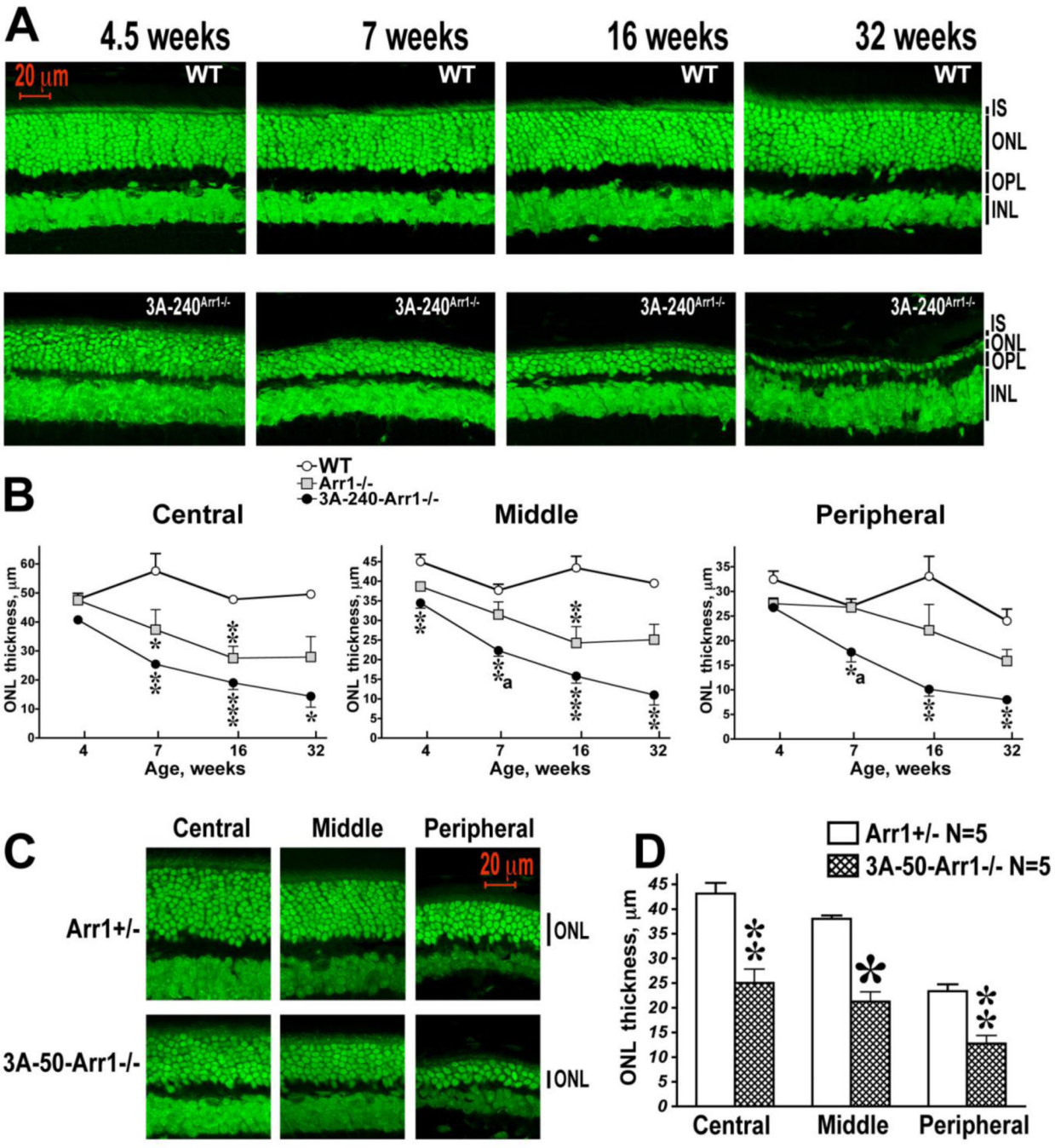

Figure 1. High expression of arrestin-1-3A mutant induces progressive severe loss of photoreceptor cells

A. Confocal images of middle retina sections of WT and 3A-240$^{arr1-/-}$ mice at indicated ages. Outer nuclear layer (ONL) was visualized by staining with green fluorescent Nissl. IS, inner segments; OPL, outer plexiform layer; INL, inner nuclear layer. Note that the layer containing photoreceptor terminals (outer plexiform layer, OPL) is also much thinner in 3A-240$^{arr1-/-}$ mice. **B.** The thickness of the ONL in the central, middle, and peripheral retina of mice at indicated ages. Two-way ANOVA with Genotype and Age as main factors revealed significant effects of Genotype in the central ($F(2,31)=43.1$, $p<0.0001$), middle ($F=64.1$, $p<0.0001$), and peripheral retina ($F=33.4$, $p<0.0001$). The effect of Age was also

significant in all retinal subdivisions ($F(3,31)=9.7$, $p<0.0001$; $F=17.4$, $p<0.0001$; $F=14.7$, $p<0.0001$ for the central, middle, and peripheral retina, respectively). The Genotype×Age interactions were also significant in the central ($F(6,31)=3,4$, $p=0.0104$), middle ($F=3.5$, $p=0.0097$), and peripheral ($F=3.2$, $p=0.0144$) retina. * - $p<0.05$, ** - $p<0.01$, *** - $p<0.001$ to wild type; a - $p<0.05$ to Arr1−/− according to Bonferroni post hoc comparison following separate one way ANOVA analysis for each retinal subdivision and age. N=3–6 mice per Genotype per Age. **C**. Confocal images of retina sections of Arr1+/− and 3A-50$^{arr1-/-}$ mice, expressing WT or mutant arrestin-1, respectively, at virtually identical levels [18, 26], at 32 weeks of age stained with green fluorescent Nissl to visualize nuclei. **D**. Quantification of the ONL thickness in the central, middle, and peripheral retina of Arr1+/− and 3A-50$^{arr1-/-}$ mice at the age of 32 weeks. * - $p<0.001$, ** - $p<0.01$ to Arr1+/−, according to Student's t-test for each subdivision.

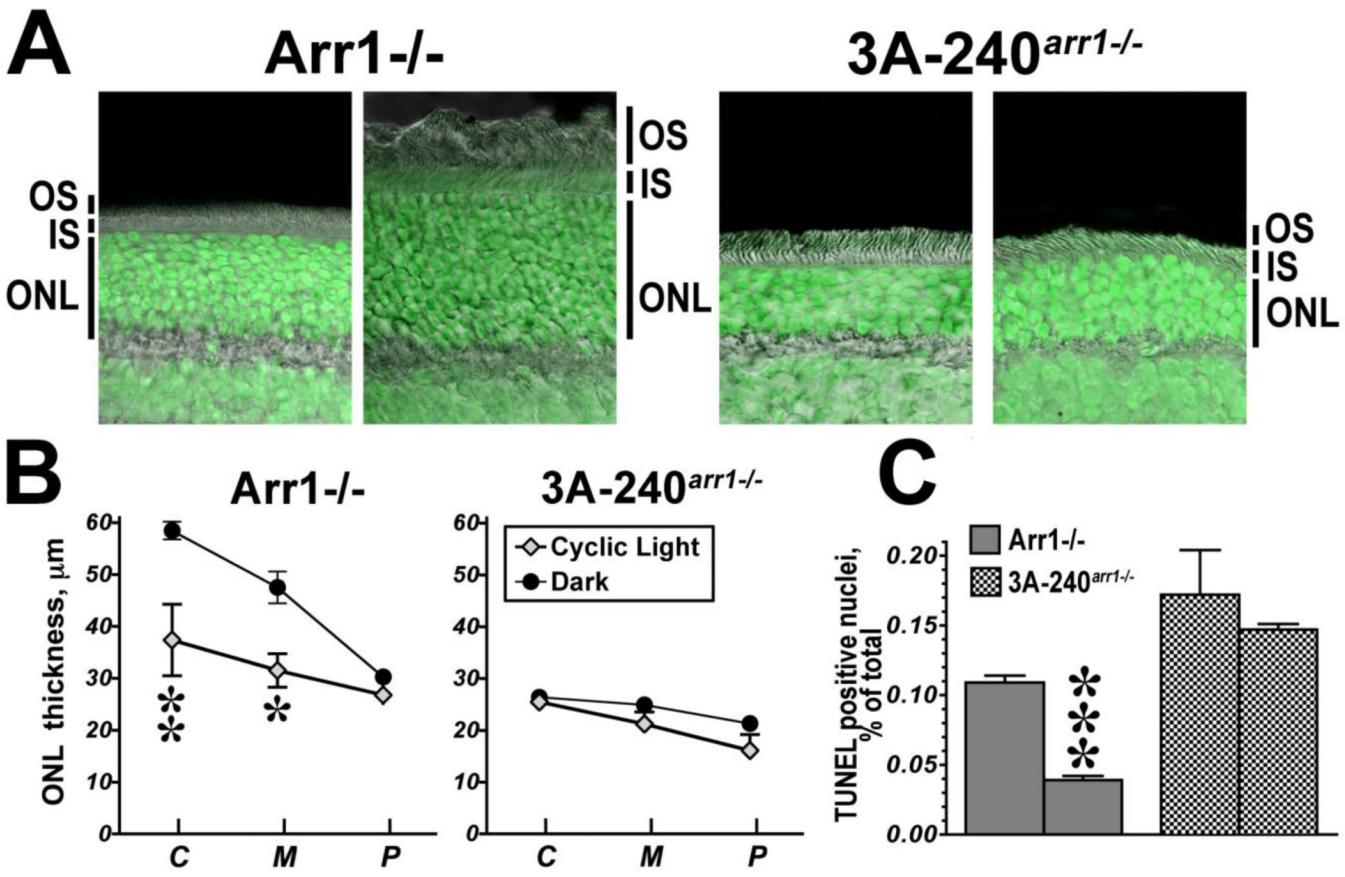

Figure 2. Photoreceptor loss in 3A-240$^{arr1-/-}$ mice is light-independent

A. Combined DIC (highlighting OS) and green fluorescent Nissl (highlighting ONL) images of the retina sections of 8 weeks old Arr1−/− and 3A-240$^{arr1-/-}$ mice. Mice were raised under cyclic light (Cyclic) or in the dark (Dark). **B.** The thickness of ONL of Arr1−/− and 3A-240$^{arr1-/-}$ mice reared in cyclic light and in complete darkness. Two-way ANOVA with Genotype and Light performed separately for each retinal subdivision C, central; M, middle; P, peripheral) yielded significant effect of Light in all subdivisions ($p<0.01$) and significant Genotype×Light interactions in the central ($p=0.007$) and middle ($p=0.0478$) but not peripheral retina. Dark rearing significantly increased the thickness of ONL in Arr1−/− mice in the central and middle retina but did not significantly affect 3A-240$^{arr1-/-}$ animals. N=3–5 mice per group. * - $p<0.05$, ** - $p<0.01$ to dark rearing in each genotype and retinal subdivision according to unpaired Student's t-test. **C.** The fraction of TUNEL-positive nuclei on the ONL of Arr1−/− and 3A-240$^{arr1-/-}$ mice (at 8 weeks) raised in cyclic light (Cyclic) or darkness (Dark), N=3 mice each. ***, $p<0.001$.

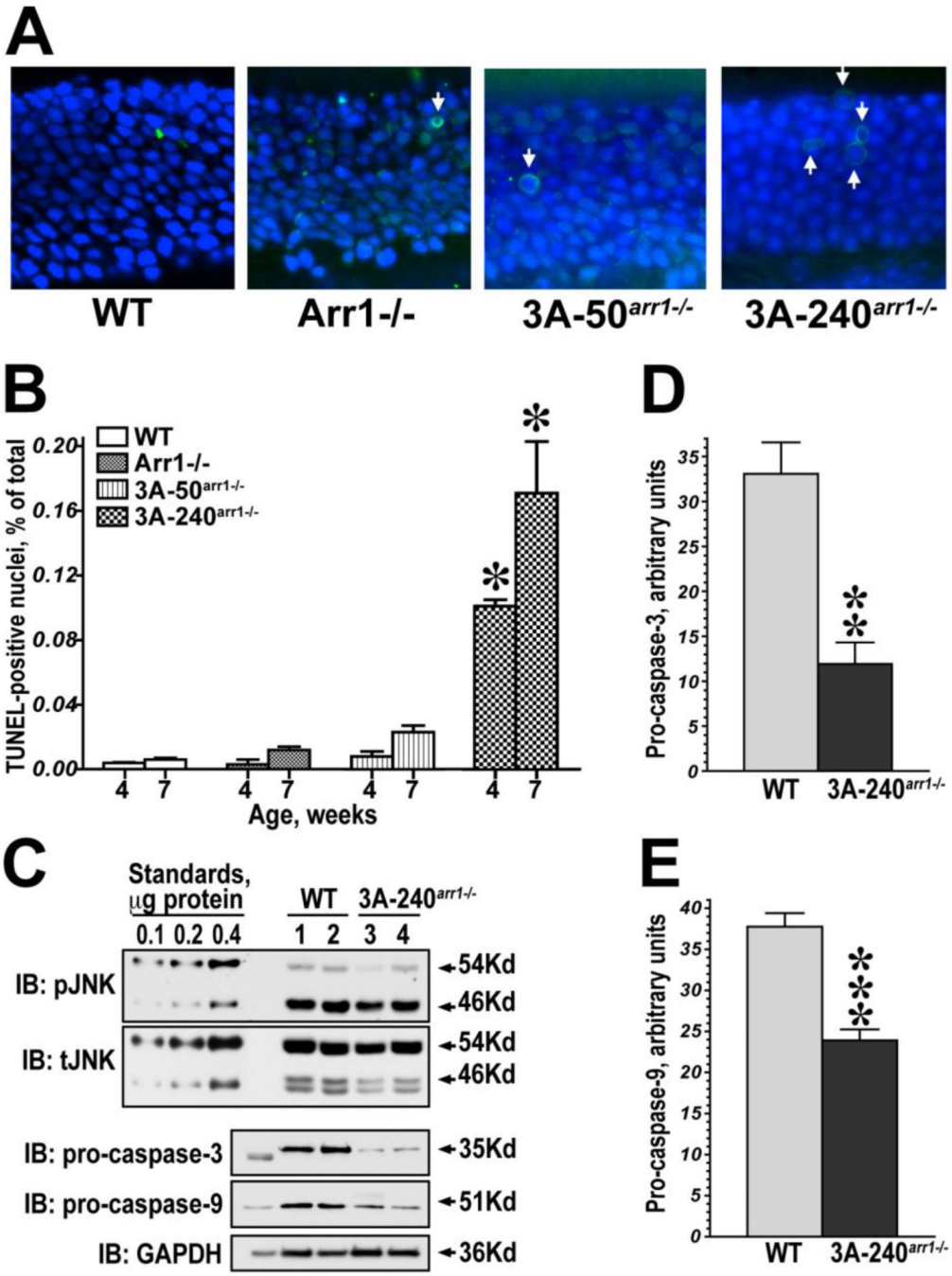

Figure 3. Photoreceptors in 3A-240$^{arr1-/-}$ animals undergo apoptotic death

A. Confocal images of TUNEL-stained (green fluorescence) retinal sections of indicated genotypes counterstained with DAPI (blue) to visualize all nuclei. TUNEL-positive apoptotic cells are indicated by arrows. **B.** The percentage of TUNEL-positive nuclei in the ONL of mice with indicated genotypes at 4 and 7 weeks. 3A-240$^{arr1-/-}$ line showed significantly higher rate of apoptosis than all other genotypes ($p<0.0001$, *) at both ages. N= 4 of 3A-240$^{arr1-/-}$ and 3 for all other genotypes per age. **C.** Western blots of whole eyecup homogenates from two representative WT (lanes 1,2) and 3A-240$^{arr1-/-}$ (lanes 3,4) animals aged 7 weeks. Top: representative Western blots showing phospho-JNK and total JNK.

Arrows indicate the molecular weights of different JNK isoforms resolved. Three left lanes show lysates of HEK293 cells (as μg protein/lane) stimulated with anicomysin (1 μM for 15 min) to induce JNK activation. No significant differences between WT and 3A-240$^{arr1-/-}$ mice were detected. The levels of pro-caspases-3 and -9 are decreased in 3A-240$^{arr1-/-}$ relative to WT (quantification shown in **D** and **E**; N=5 for WT and N=4 for 3A-240$^{arr1-/-}$) (* - $p<0.05$, **, $p<0.01$). GAPDH was used as loading control. Lysate of HEK293 cells (0.4 μg of total protein) was run on the leftmost lane on each blot. The molecular weights of corresponding bands are shown on the right.

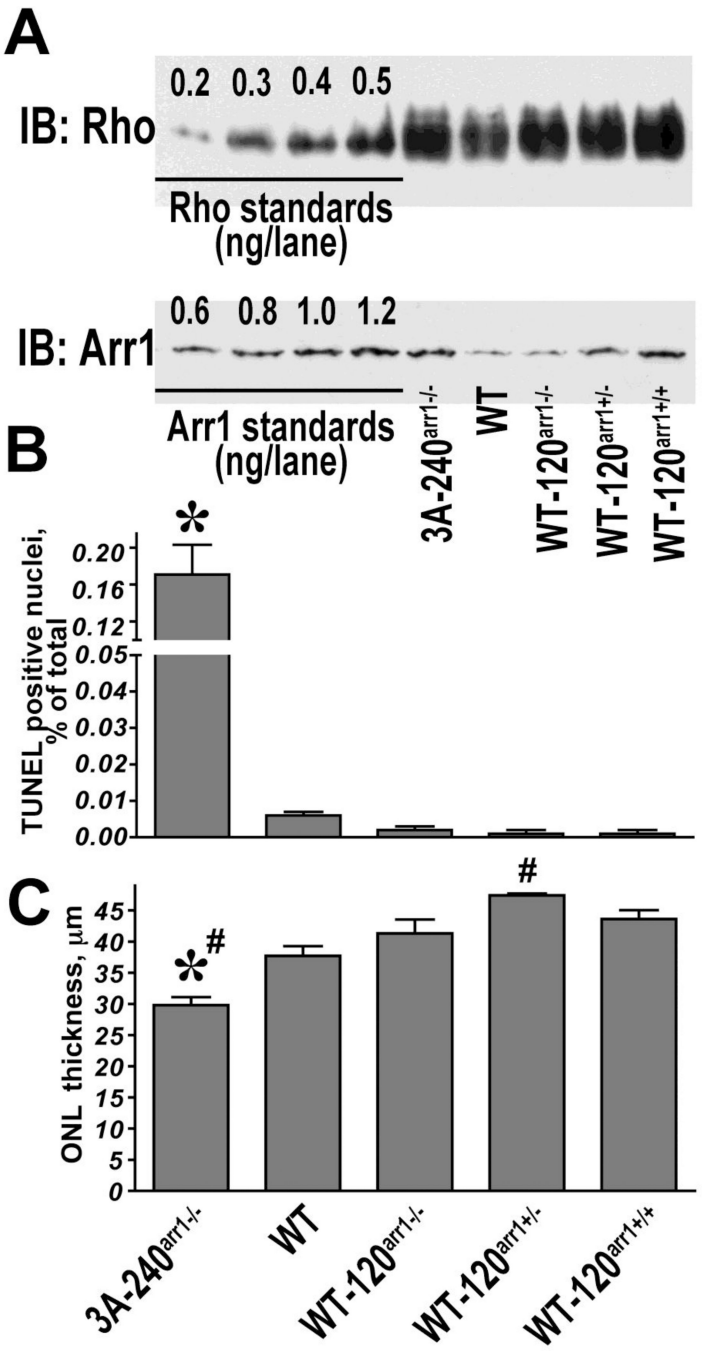

Figure 4. High expression of WT arrestin-1 is harmless

A. Western blot of rhodopsin (Rho) and arrestin-1 (Arr1) in eyecups of indicated mouse lines. Indicated known amounts of corresponding purified proteins were run alongside samples as standards. **B,C**. Comparison of the rate of photoreceptor apoptosis (**B**) and the thickness of the ONL (**C**) among different genotypes at 7 weeks. Note that high expression of WT arrestin-1 in WT-120 lines did not significantly change the rate of apoptosis, as compared to WT (* - $p<0.001$ to all lines by Bonferroni-Dunn following one-way ANOVA). 3A-240$^{arr1-/-}$ mice have significantly thinner ONL than all other genotypes. Among mice

expressing WT arrestin-1, WT-120$^{arr1+/-}$ had significantly thicker ONL than WT. N=3–4 mice per group. (* - $p<0.001$ to WT-120 lines, # - $p<0.01$ to WT)

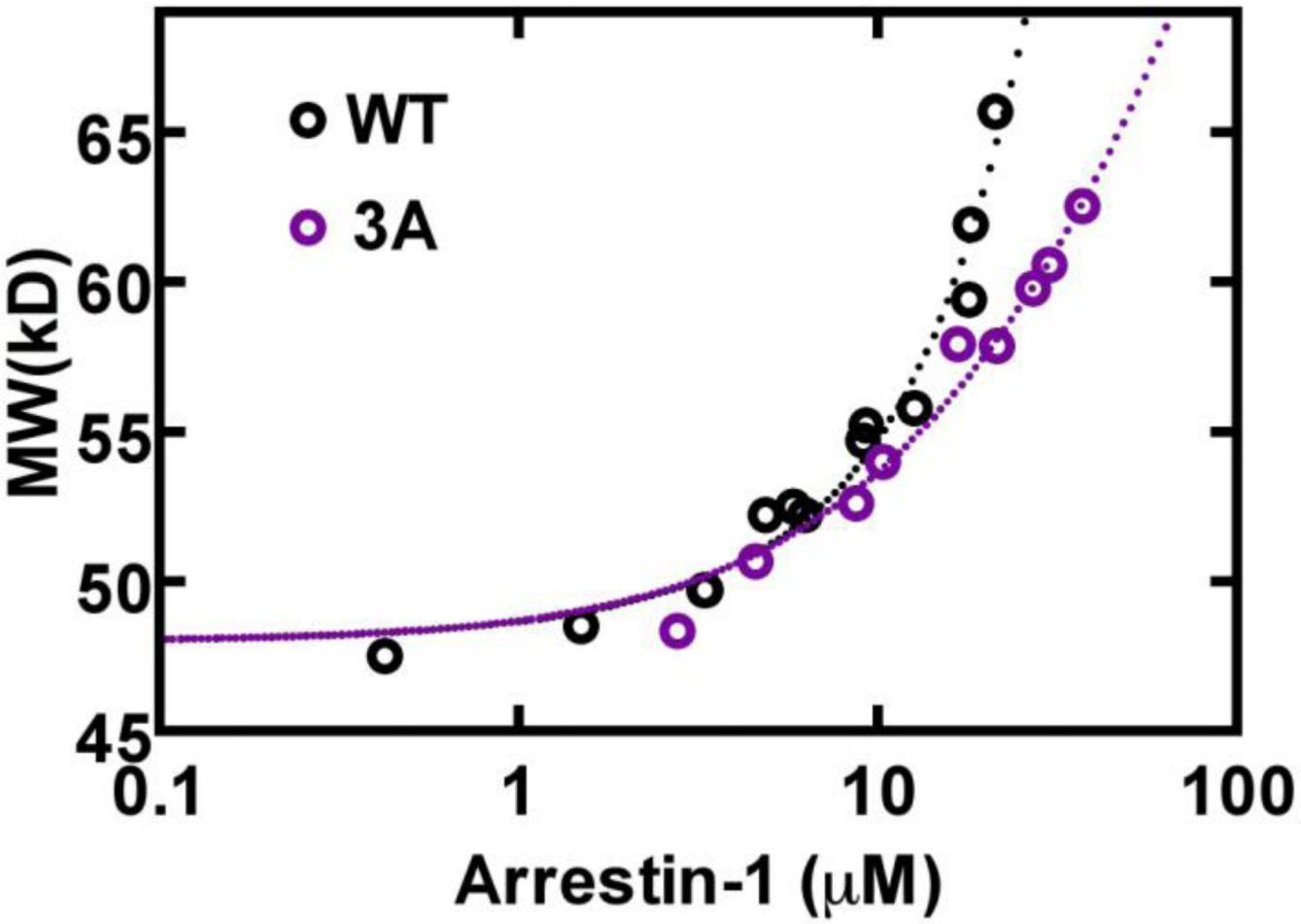

Figure 5. Impaired self-association of mouse arrestin-1-3A

The average molecular weight of WT mouse arrestin-1 (black) and arrestin-1-3A mutant (purple) as a function of total concentration was determined from the light scattering data as described in the Methods. Dotted curves are least-squares fits of the data to the MDT model [21] with the following parameters: WT, $K_{D,dim}$ = 57.5±0.6 μM and $K_{D,tet}$ = 63.1±2.6 μM; arrestin-1-3A, $K_{D,dim}$ = 135±2 μM and $K_{D,tet}$ = 380±79 μM.

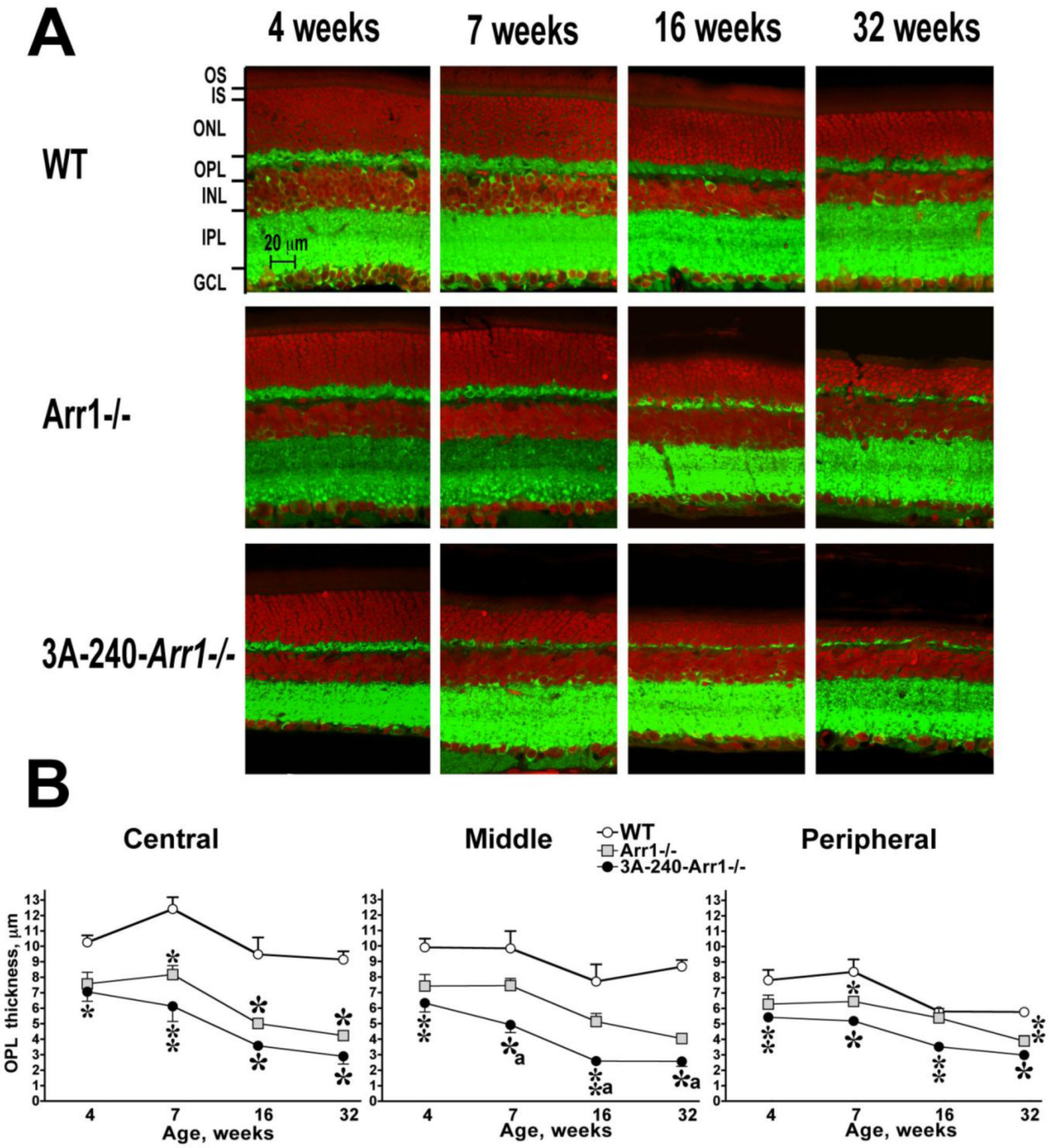

Figure 6. High expression of arrestin-1-3A mutant induces progressive loss of photoreceptor synaptic terminals

A. Confocal images of middle retina sections of WT, Arr1−/−, and 3A-240$^{arr1-/-}$ mice at indicated ages. Outer (OPL) and inner (IPL) plexiform layers are stained by antibody to presynaptic terminal marker NSF (green). Nuclear layers are counterstained with red fluorescent Nissl. IS, inner segments; OPL, outer plexiform layer; INL, inner nuclear layer. **B**. Measurement of the thickness of the NSF-stained OPL in the central, middle, and peripheral retina of mice at indicated ages. Two-way ANOVA with Genotype and Age as main factors revealed significant effects of Genotype in the central ($F(2,39)=53$, $p<0.0001$), middle ($F=55.7$, $p<0.0001$), and peripheral retina ($F=34$, $p<0.0001$). The effect of Age was

also significant in all retinal subdivisions ($F(3,39)=16.3, 16.9, 23$, $p<0.0001$, for the central, middle, and peripheral retina, respectively), but there was no significant Genotype×Age interactions ($p>0.05$). Bonferroni-Dunn post hoc comparison across ages showed significant difference between Arr1−/− and 3A-240$^{arr1-/-}$ in the middle ($p<0.01$) and peripheral ($p<0.05$) but not in the central retina. N=3–6 mice per genotype per age. * - $p<0.005$, ** - $p<0.001$, *** - $p<0.001$ to WT; a - $p<0.05$ to Arr1−/− according to Bonferroni-Dunn post hoc comparison following separate one way ANOVA analysis for each retinal subdivision and age.

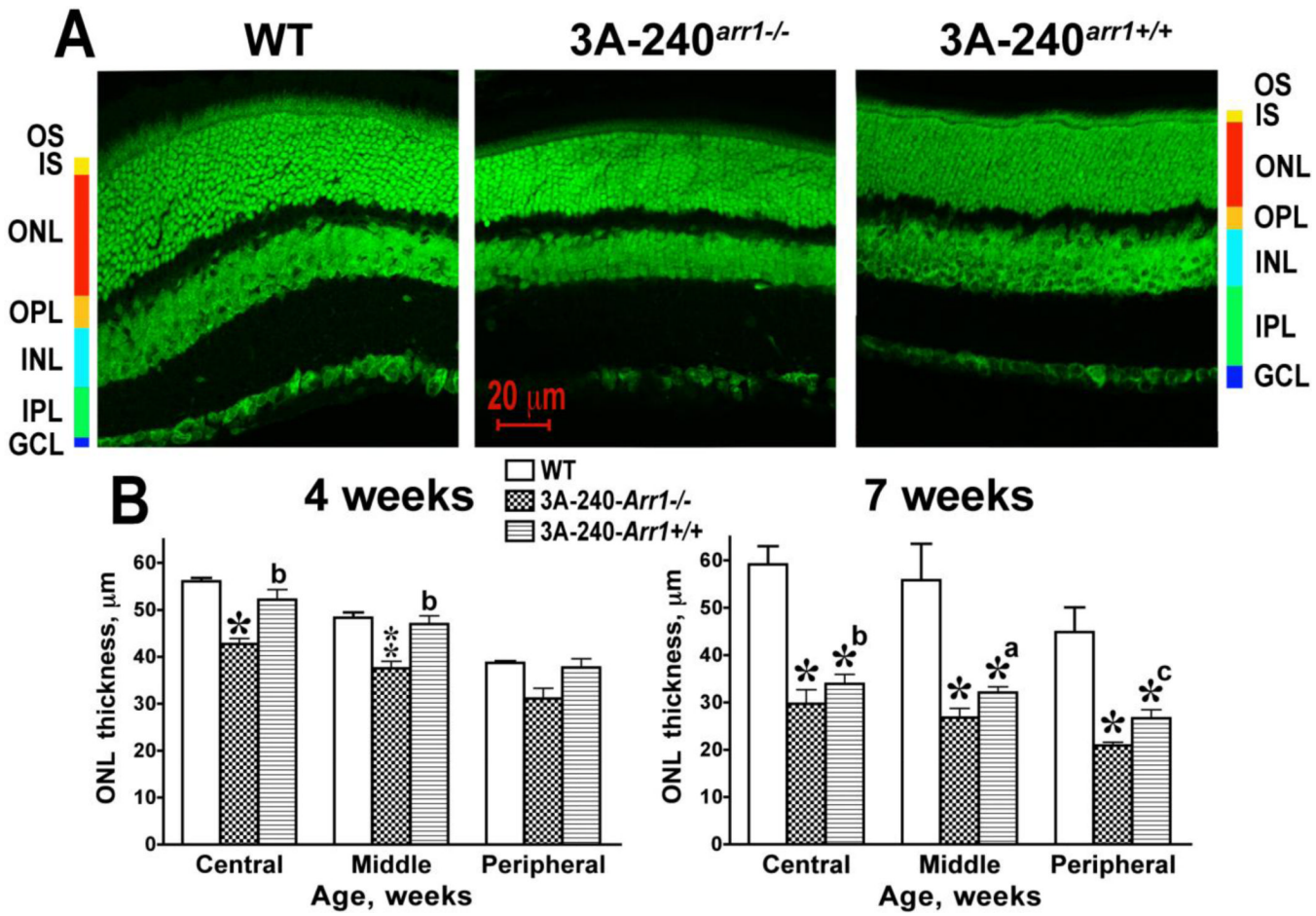

Figure 7. Co-expression of WT arrestin-1 protects photoreceptors in 3A-240$^{arr1-/-}$ mice

A. Confocal images of the middle retina of 4 week-old mice stained with green fluorescent Nissl demonstrating photoreceptor protection in mice expressing 3A-240 on Arr1+/+ background. **B**. Comparison of ONL thickness in central, middle, and peripheral retina at indicated ages in WT, 3A-240$^{arr1-/-}$ and 3A- 240$^{arr1+/+}$ animals. Data analysis by one-way ANOVA with Genotype as main factor separately for each age and retinal subdivision revealed significant effect of Genotype at both ages in all retinal subdivisions (at 4 weeks in the peripheral retina there were no individual differences with $F(2,13)=4.93$, $p=0.0255$). Post hoc analysis demonstrated that at the earlier age only 3A-240$^{arr1-/-}$ was significantly different from control, whereas at 7 weeks of age both 3A-240$^{arr1-/-}$ and 3A-240$^{arr1+/+}$ were significantly impaired as compared to WT. However, even at 7 weeks ONL in 3A-240$^{arr1+/+}$ was significantly thicker than in 3A-240$^{arr1-/-}$ in all retinal subdivisions. N=6–9 mice per group. * - $p<0.05$, ** - $p<0.01$, *** - $p<0.001$ to WT; a - $p<0.05$, b - $p<0.01$, c - $p<0.001$ to 3A-240$^{arr1-/-}$ according to Bonferroni-Dunn post hoc comparison.

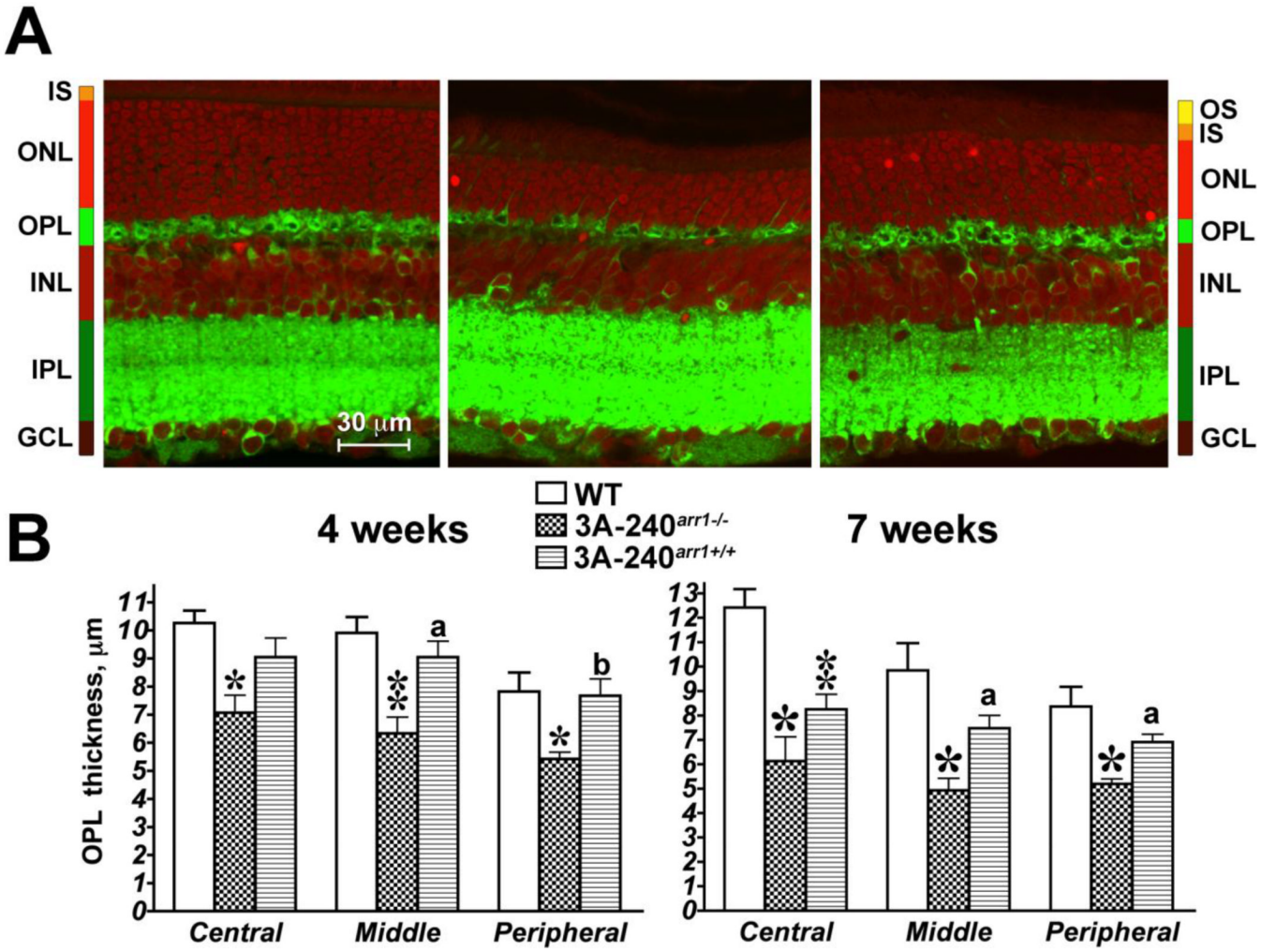

Figure 8. Co-expression of WT arrestin-1 protects photoreceptor synaptic terminals in 3A-240 mice

A. Confocal images of middle retina sections of WT, 3A-240$^{arr1-/-}$ and 3A-240$^{arr1+/+}$ mice at 7 weeks. Outer plexiform layer (OPL) was visualized by immunohistochemistry for NSF (green). Nuclear layers are counterstained with red fluorescent Nissl. **B.** Comparison of OPL thickness in central, middle, and peripheral retina at indicated ages in WT, 3A-240$^{arr1-/-}$ and 3A-240$^{arr1+/+}$ animals. Data analysis by one-way ANOVA with Genotype as main factor separately for each age and retinal subdivision revealed significant effect of Genotype at both ages in all retinal subdivisions ($p<0.01$ for 4 weeks and $p<0.001$ for 7 weeks). N= 5 mice per genotype per age. * - $p<0.05$, ** - $p<0.01$, *** - $p<0.001$ to WT; a - $p<0.05$, aa - $p<0.01$ to 3A-240$^{arr1-/-}$ according to Bonferroni-Dunn post hoc comparison.